To appear in the *Combustion Science and Technology*

Vol. 00, No. 00, Month 20XX, 1–28

Experimental Investigation of the Effect of Steam Dilution on the Combustion of Methane for Humidified micro Gas Turbine Applications

Ward De Paepe[a*], Parisa Sayad[b], Svend Bram[c], Jens Klingmann[b] and Francesco Contino[a]

[a] *Vrije Universiteit Brussel (VUB), Department of Mechanical Engineering (MECH), Brussels, Belgium*;

[b] *Lund University, Department of Energy Sciences, Lund, Sweden*

[c] *Vrije Universiteit Brussel (VUB), Department of Engineering Technology (INDI), Brussels, Belgium*

Water introduction in the micro Gas Turbine (mGT) cycle is considered the optimal route for waste heat recovery and flexibility increase of such small-scale Combined Heat and Power (CHP) unit. However, humidification of the combustion air in a mGT affects combustion stability, efficiency and exhaust gas emissions. This can lead to a non-stable, incomplete combustion, which will affect the global efficiency negatively. Additionally, CO emissions will increase. The non-stable, incomplete combustion might result in an engine shutdown due to a flameout. To study the impact

*Corresponding author. Email: wdepaepe@vub.ac.be

of humidification on the combustion of methane in a humidified mGT, we performed combustion experiments in an atmospheric, variable-swirl, premixed combustion chamber. The results of these experiments are summarized in this paper. The effect of the humidification of the combustion air was simulated by adding steam to the combustion air. The impact of the steam injection on methane combustion has been studied at variable swirl number and steam fraction. Experimental results showed a linearly increasing Lean Blowout (LBO) equivalence ratio for methane combustion with increasing steam fraction. In addition, CO emission levels started to rise at higher equivalence ratio for higher steam fractions compared to combustion under dry conditions. The CO emission levels at stable combustion were however still same order of magnitude as for the dry combustion. The swirl number has little effect on the LBO limit. Final results indicated the possibility to maintain complete and stable combustion under humidified conditions with low CO emissions at higher equivalence ratio compared to the dry combustion.

Keywords: Steam injection; combustion stability; Lean Blowout (LBO) limit; exhaust gas emissions; atmospheric, variable-swirl, premixed combustion chamber

1. Introduction

Micro Gas Turbines (mGTs) offered great opportunities for small-scale Combined Heat and Power (CHP) production (Pilavachi, 2002). In addition, mGTs have several advantages over their major competitors in the same power range (up to 500 kW_e), the Internal Combustion Engines (ICEs): a small number of moving parts, compact size and light weight, lower emissions and lower electricity costs (U.S. Department of Energy, Office of Energy Efficiency & Renewable Energy, Office of

Power Technologies, 2000). However, mGTs never fully penetrated the CHP market (Frost & Sullivan, 2011). The main reason for the lack of success of the mGTs is their low electric efficiency (typically 30% (McDonald, 2000)). Due to the low electric efficiency, the mGT is forced to operate according to the heat demand. A low heat demand mostly leads to a forced shutdown, since taking the necessary power from the grid is less expensive than the electricity production cost of the mGT in pure power production mode. This forced shutdown reduces the total amount of yearly running hours, making the investment less attractive (Delattin, Bram, Knoops and De Ruyck, 2008). Introducing water in the mGT cycle in between compressor outlet and recuperator inlet is the optimal solution for the recuperation of the lost thermal power (De Paepe, Delattin, Bram and De Ruyck, 2013). By converting the mGT into a micro Humid Air Turbine (mHAT), electric efficiency can be increased by 6.7 % relative. Parente, Traverso and Massardo (2003) calculated that converting the mGT into a mHAT would reduce the specific capital cost up to 14 %.

Additional water or steam in the combustion air will however effect the combustion in the mGT. Exhaust gas emissions, the combustion stability and efficiency will be affected by the water or steam injection. This can lead to a non-stable, incomplete combustion, which will affect the global efficiency negatively. Additionally, CO emissions will increase. The non-stable, incomplete combustion might result in an engine shutdown due to a combustion flameout. The effects of humidification on the combustion (change in emissions, mainly NO_x and CO, combustion stability and efficiency) have been studied in the past. A short overview of the recent research covering these issues is given in the following paragraphs.

Water or steam injection in Gas Turbine (GT) cycle reduces the NO_x levels. Chen, Maloney and Day (2004) measured a 90% NO_x reduction by adding 10 % humidity to the compressed air compared to the dry GT cycle when using a liquid fuel in a diffusion flame combustor for the Humid Air Turbine (HAT). Belokon, Khritov, Klyachko, Tschepin, Zakharov and George Opdyke (2002) saw a similar

trend for methane combustion in a diffusion flame combustor, also for the HAT cycle. For premixed combustion of natural gas, Day, Kendrick, Bhargava, Sowa, Colket, Casleton and Maloney (1999) also noticed that moisture in the feed stream reduces NO_x emissions. According to Dryer (1977), the NO_x emissions in natural gas combustion are influenced in two ways: a physical and a chemical way. First, the flame temperature is lower, which will reduce the formation of thermal NO_x. Secondly, the steam addition will change the concentrations of the O, OH and H species (Mazas, Lacoste and Schuller, 2010). Since these species are also involved in the formation of NO_x, they will influence the final NO_x exhaust. These effects have been studied by different researchers, however the influence of water on NO_x formation has been reported differently. Zhao, Yamashita, Kitagawa, Arai and Furuhata (2002) noticed that for a natural gas diffusion flame, the additional steam leads to higher thermal NO_x emissions. Total NO_x emissions were however lower due to a significantly lower prompt NO_x. This however contradicts with the finding of Göke, Füri, Bourque, Bobusch, Göckeler, Krüger, Schimek, Terhaar and Paschereit (2013). According to Bhargava, Colket, Sowa, Casleton and Maloney (2000), the lower NO_x in humid air premixed combustion is a result of the higher OH radical concentration. They however did not investigate the effect of pressure on the NO_x emissions. Both Day et al. (1999) and Kobayashi, Yata, Ichikawa and Ogami (2009) showed that the NO_x emissions become higher with increasing pressure, but Kobayashi et al. (2009) also indicated that this effect becomes weaker with increasing steam fraction. Recently, Göke, Schimek, Terhaar, Reichel, Göckeler, Krüger, Fleck, Griebel and Paschereit (2012) revealed numerically that reduced NO_x emissions are mainly caused by lower concentrations of atomic oxygen at steam-diluted conditions, constraining the thermal pathway.

The different studies in literature on exhaust gas emissions show no clear trend for the CO levels under steam injection conditions. CO levels seem to depend on the operating conditions and the combustor layout. Park, Keel and Yun (2007)

indicated that CO is slightly reduced by steam injection, while in their studies, Day et al. (1999) and Göke et al. (2012) indicated no significant effect of steam injection on the CO levels. Both however showed that CO emissions reduce with increasing pressure.

In literature, less studies exist on the combustion efficiency. Belokon et al. (2002) developed a method to predict the combustion efficiency and NO_x levels for diffusion flame combustors for HAT applications. Hermann, Klingmann and Gabrielsson (2003) indicated that richer combustion is required to keep the combustion efficiency (thus CO emissions) at a tolerable level using premixed flames. Therefore, although NO_x emissions strongly reduce by the addition of water in a combustion chamber with premixed flame, this decrease will vanish.

In this paper, we will present the results of combustion experiments performed with steam injection. The experiments were performed in the atmospheric, variable-swirl, premixed combustor of the Thermal Power Engineering division of the Department of Energy Sciences of Lund University, Sweden. In this study, we focused on the Lean Blowout (LBO) limit and CO emissions of methane combustion, since the effect of steam addition on NO_x emissions is already well-known. In addition, mGTs use low NO_x premixed combustors, resulting in very low emissions (for instance, less then 15 ppm at full load for the Turbec T100 mGT (Turbec AB, 2000-2001)). In the mHAT case, water is added to the cycle to enhance the mGT performance, not to reduce NO_x levels. By measuring the LBO limit, we tried to predict how the fuel control of the mGT needs to be changed in order to get a stable combustion under humid conditions. CO emission levels were measured to show the influence of the steam dilution on the exhaust emissions. Out of these results, guidelines for combustion in humidified mGTs will be formulated.

The combustion experiments performed for and discussed in this paper are similar to the experiments performed by Göke et al. (2012). The major difference between both experiments however is the swirl number. For their experiments, Göke et al.

(2012) used a swirl number of 0.9. A typical mGT combustor, like the Turbec T100 mGT combustor, has however a lower swirl number of 0.6. Since the swirl number has an impact on LBO limit (Sayad, Schönborn, Clerini and Klingmann, 2012), we decided to perform steam dilution experiments at swirl numbers closer to the T100 mGT swirl number. This allowed for a more accurate discussion on the effect of air humidification on the combustion in the Turbec T100 mGT.

This Turbec T100 mGT combustor is a typical lean premixed combustor (Figure 1). The combustor is a reverse-flow, tubular combustor composed out of a liner and an inner flame tube (Figure 2). A detailed description of the different parts and the operation of the combustor is presented by Calabria, Chiariello, Massoli and Reale (2015). Different researchers studied in this combustion chamber the effect of alternative fuels or higher CO_2 levels on the combustion, showing the potential to achieve high performance in off-design conditions (Cadorin, Pinelli, Vaccari, Calabria, Chiariello, Massoli and Bianchi, 2012; Cameretti, Piazzesi, Reale and Tuccillo, 2009; Cameretti, Reale and Tuccillo, 2006; Cameretti and Tuccillo, 2014). Studies on humidified combustion have however not yet been presented for this combustor, which indicates the importance of the experiments presented in this paper.

In the following sections of this paper, we will first discuss the experimental approach and provide more details about the atmospheric, variable-swirl, premixed combustor and steam generator. Additional information concerning the experimental procedure and the exhaust gas emissions measurement is also given in this section. In the second section, the results of the LBO experiments are shown and discussed together with the CO emissions results. The effect of the different variations in the inlet conditions – steam ratio and swirl number – on the results is discussed. The experimental results are also linked with actual mGT combustion chambers. In addition to the experimental results, simplified equilibrium and chemical kinetic calculations concerning adiabatic flame temperature at equilibrium in `GASEQ` and

CO emissions values in OpenSMOKE++ have been added to this study. Finally, a conclusion about the experiments and guidelines for humidified mGT combustion control are presented.

2. Experimental approach for combustion experiments

For the combustion experiments, an atmospheric, variable-swirl, premixed burner with a circular cross section was used in combination with an electric steam generator. The used burner is a modified version of the burner used to investigate the effect of dilution, mass flow rate, swirl number and inlet air temperature on the LBO limit of methane (Sayad et al., 2012) and different syngas mixtures (Sayad, Schönborn and Klingmann, 2013) combustion.

In the following subsections, the experimental set-up, consisting out of the burner and the steam generator, is discussed. In addition, the used experimental procedures for LBO limit determination and CO emissions measurements are given.

2.1. *Burner*

The experiments were carried out in an atmospheric, variable-swirl, premixed burner with circular cross section (Figure 3). The burner has a total length of 350 mm and an inner diameter of 63 mm. A quartz tube with the same inner diameter as the burner provides optical access to the first 120 mm of the flame, enabling the visual detection of LBO.

A swirling flow of air and methane was supplied to the combustor through a centrally located premixing tube. This tube has a diameter of 15 mm and a total length of 80 mm of which the last 50 mm consists of a quartz tube. This quartz tube allows the detection of possible flashback in the premixing tube.

Both axial and tangential air flows are combined in the swirler, located at the entrance of the premixing tube. The swirler allowed for the introduction of air into

the premixing tube in axial and tangential directions in varying proportions. Before entering the swirler, the axial flow is passed through a flow straightener, while the tangential flow passes through four channels of 3 mm wide and 10 mm high.

The swirl number of the flow entering the combustor was varied by changing the proportion of tangential to axial flow through the swirler. Axial and tangential flows were measured and preheated individually using two laminar-flow, differential-pressure mass-flow controllers (Alicat MCR250) and feedback-controlled air heaters (Sylvania Sureheat Jet) of 8 kW power. In order to make sure that the equivalence ratio (Φ) of the fuel-air mixture entering the combustor was the same in both axial and tangential directions, the axial and tangential air flows can be separately premixed with fuel upstream of the swirler. A laminar-flow, differential-pressure mass-flow controller (Alicat MCR50) can be used to split and control the fuel flow based on the ratio between the tangential and axial air mass flow rates.

Ahead of this splitting mass-flow controller, the desired methane fuel flow was generated by a laminar-flow differential-pressure mass-flow controller (Alicat MCR50). CH_4 (purity 99.98 %) was supplied from gas bottles. The exhaust gases from the combustor were discharged into a force-ventilated extractor hood. A scheme of the burner cross section and the details of the geometry are shown in Figure 4.

As mentioned before, the mass flow rate of the axial and swirl component of the air can be changed. Depending on the relation between the strength of the two components, different flow patterns will emerge in the combustor. In order to quantify this relation, the swirl number can be defined as (Syred and Beér, 1974):

$$S = \frac{G_\mathrm{t}}{R_\mathrm{S} G_\mathrm{a}}, \tag{1}$$

where R_S is the radius of the swirler, G_t the axial flux of the tangential momentum and G_a the axial flux of the axial momentum. These fluxes can be calculated as

follows:

$$G_{\mathrm{t}} = 2\pi \int_0^{R_{\mathrm{S}}} \rho U W r^2 \mathrm{d}r, \tag{2}$$

$$G_{\mathrm{a}} = 2\pi \int_0^{R_{\mathrm{S}}} \rho U^2 r \mathrm{d}r, \tag{3}$$

where ρ is the density of the gas, U the axial velocity, W the tangential velocity and r the radius of the swirler exit.

To determine the swirl number for each flow condition, the axial and tangential velocity profiles were measured 1 mm above the dump plane of the combustor using Laser Doppler Anemometry (LDA). A detailed description of the used equipment and measured flow patterns can be found in Sayad et al. (2013).

2.2. *Steam boiler*

Steam was produced using an electric steam generator. Rather than using a pressurised steam boiler containing a two-phase mixture of boiling water and saturated steam, we opt for a direct-through steam generator in order to avoid safety issues. Water was routed through an electric heated metal block. The metal block was heated by 10 low-density cartridge heaters (*Omega* LDC00261) each providing up to 300 W electrical power. By routing the water over multiple passes through the block, the water was heated, converted into steam and superheated. The heat flux was controlled by setting the block temperature rather than controlling the steam temperature. The thermal inertia of the heater block was too large to use a fast changing parameter like the steam temperature to control the heat flux. Once an equilibrium was reached between the ingoing heat flux, the outgoing steam flow and the heat losses, the steam temperature would remain constant. This however required a constant steam mass flow rate. Rather than directly controlling the steam mass flow rate, we controlled the water mass flow rate using a precision water flow meter and controller (Alicat LC-500-CCM) with a maximal flow rate of 20 kg/h

and an accuracy of 2 % of the full scale. We opt for controlling the water flow rate, since it allows much more accurate flow rate control than typical steam flow controllers. The steam was mixed upstream of the swirler with the air flows where the fuel was added. Final injection temperature of the steam varied between 180 °C and 250 °C. This difference in temperature could be compensated by adjusting the feedback-controlled air heaters in order to keep the inlet air temperature of the burner constant.

2.3. *LBO test procedure*

The focus of the presented work was the investigation of the effect of steam dilution on the LBO limit for methane combustion at different swirl numbers and steam fractions. The swirl number was changed from 0.66 to 0.53. Tests were only performed at high swirl numbers, which are representative for mGT combustion chambers. Initially, the total volume flow rate of air was kept constant and equal to 200 slpm[1] for both $S = 0.66$ (200 slpm swirl and 0 slpm axial flow) and $S = 0.53$ (150 slpm swirl and 50 slpm axial flow) swirl number. The power of the electric steam boiler was limited, resulting in a maximum possible steam fraction of 18 % for a given air volume flow rate of 200 slpm. Currently, GT cycle developers are looking towards higher humidity levels (up to 30 %) for ultra-wet combustion. To reach this high steam fraction, the air volume flow rate was lowered till 125 slpm to be able to reach 28 % steam fraction at a swirl number of $S = 0.66$. By lowering the air mass flow rate, experiments could be performed at higher steam ratios. Lowering the mass flow rate will however slightly effect the LBO limit, as has been indicated in Sayad et al. (2012).

For the $S = 0.53$ swirl case, in ideal conditions, fuel and steam would be mixed separately in the axial and the swirl flow to get fully premixed air and the same

[1] slpm = standard litre per minute

steam ratio in both axial and swirl flow (as described in the previous section). Due to control issues, it was not possible to maintain a constant steam and fuel flow rate when using the splitter. Therefore, we decided to inject the steam and fuel in the swirl flow (largest fraction).

All tests were performed at atmospheric pressure. The inlet air temperature of the burner was kept constant at 650 K in order to exclude the effect of inlet air temperature variations. Previous experiments, performed by Sayad et al. (2012), indicated that changing the inlet temperature by 200 K will reduce the LBO equivalence ratio by 0.10. The inlet air temperature was controlled by adjusting the air heaters and measuring the temperature in the centre of the inlet before and after the experiments using a K-type thermocouple.

To the author's knowledge, no standard procedure for LBO-limit determination exists. Therefore, the same procedure that was used in Sayad et al. (2012) and Sayad et al. (2013) for LBO-determination of methane and syngas on the same test rig, has been used. This procedure is similar the one presented by (Xiao and Huang, 2015). At the different steam fraction, a rich mixture (equivalence ratio close to 1) was ignited. At very high steam fractions (28 %), additional H_2 was added to the fuel for better ignition. Once the mixture was ignited, the H_2 flow was cut. After ignition, the equivalence ratio was reduced slowly from $\Phi = \Phi_{\text{init}}$ until LBO occurred at $\Phi = \Phi_{\text{LBO}}$ by gradually reducing the methane fuel flow rate. After each change of the fuel flow rate, it was maintained constant for at least 3 minutes to stabilize the flame and to allow the combustion chamber to reach thermal equilibrium. The fuel flow rate was reduced until blowout occured. For each steam fraction, this procedure was conducted three times, to show repeatability of the experiments and to exclude possible deviations due to sudden instabilities in one of the flows.

2.4. *CO emissions measurements*

CO emissions were captured for each swirl number at different equivalence ratios and steam injection ratios. A sample of the flue gases was taken above the metal liner (Figure 3). The sampling device consisted out of a metal tube with different openings along the burner radius, in order to get a representative sample of the total exhaust gas emissions. The water in the flue gases was condensed before entering the CO measuring device (a Rousemount Binos). The device was calibrated on a daily basis and compensated for the changing atmospheric pressure. The maximal CO concentration that could be measured was 950 ppm with an accuracy below 1 % of the full scale at constant temperature and pressure. Finally, the CO emissions were measured and averaged over a period of 3 minutes in which the steam flow rate and equivalence ratio were kept constant.

3. Results of the combustion experiments

In this section, we will discuss the effect of steam dilution on methane combustion observed during the steam injection combustion experiments, with special focus on the LBO limit and CO emissions, linked to mGT combustors. The steam fraction Ω, used in this section, is defined as follows:

$$\Omega = \frac{\dot{m}_{\text{steam}}}{\dot{m}_{\text{air,dry}}}, \tag{4}$$

while the equivalent fuel-air ratio Φ is always defined in dry air:

$$\Phi = \left(\frac{\dot{m}_{\text{fuel}}}{\dot{m}_{\text{air,dry}}}\right) \Big/ \left(\frac{\dot{m}_{\text{fuel}}}{\dot{m}_{\text{air,dry}}}\right)_{\text{Stoichiometric}}. \tag{5}$$

In following subsections, we will first discuss the effect of steam dilution on the LBO limit of methane combustion in the atmospheric, variable-swirl, premixed burner. In the next subsection, the effect of steam addition to the combustion air on the CO emissions is discussed. Finally, the experimental results will be linked

with the Turbec T100 mGT combustor.

3.1. *Effect of steam dilution on the LBO limit*

Increasing the steam fraction will increase the LBO equivalence ratio for methane combustion (Figure 5). For both swirl numbers of $S = 0.66$ and $S = 0.53$ and total air volume flow rates of 200 slpm and 125 slpm, the increase in LBO equivalence ratio is linear. For the same mass flow rate, the difference between the LBO equivalence ratio for swirl numbers $S = 0.66$ and $S = 0.53$ is rather small. This is in accordance with previous experiments, where Sayad et al. (2012) indicated that the differences in LBO equivalence ratio between high swirl numbers (0.66 and 0.53) are rather small. Lowering the swirl number will lead to an increasing LBO equivalence ratio. The deviations in the measurements can be explained by the uncertainty on the steam and fuel mass flow rates. Decreasing the air mass flow rate slightly increases the LBO limit, which is also in accordance with previous experiments. Sayad et al. (2012) indicated that for air flow rates lower than 200 slpm, the LBO limit increases with decreasing mass flow rate.

The increasing LBO equivalence ratio from Figure 5 is a result of the increasing steam fraction. The presence of the steam in the combustion air will absorb heat of the combustion. This results in lower flame temperature, enabling LBO at higher equivalence ratio, which explains the increasing LBO equivalence ratio.

Broadband luminosity photographs of the flame illustrate the changing flame shape when decreasing the equivalence ratio under dry conditions (Figure 6) and wet conditions (Figure 7) during LBO experiments. During previous experiments studying the LBO limit at various swirl numbers, three distinct categories of blowout were observed. These could be classified as low swirl ($S \approx 0.03$), moderate swirl ($S \approx 0.28$) and high swirl ($S \approx 0.60$) cases (Sayad et al., 2013). LDA measurements taken during these previous experiments clearly showed the existence of an inner and outer recirculation zone in the flow at high swirl numbers. Similar observations

at the same swirl numbers (0.66 and 0.53) were made during the experiments presented in this paper (Figure 7).

At ignition equivalence ratio, the dry flame is very short, attached to the inlet (Figure 6(a)). The flame is concentrated around the inner recirculation zone, resulting in a heart-like shape. When the equivalence ratio is reduced, the flame starts to oscillate between the initial position around the inner recirculation zone and the outer recirculation zone. This behaviour is the result of the existence of the two circulation zones. At the transition zone between these two positions, the combustion becomes very unstable. This gives rise to very heavy vibrations and a loud noise. These instabilities even lead to flameout. For the determination of the LBO limit, the equivalence ratio needed to be lowered faster, in order to quickly transit through this transition zone, lacking the time to take a photograph. When the equivalence ratio is reduced further (reducing the fuel flow rate), the flame becomes detached from the burner and moves to a stable lifted position (Figure 6(b)). Further reducing the equivalence ratio will keep the flame in its lifted position, but will make the flame progressively thinner and elongated until blowout occurs very smoothly.

During experiments with steam injection, the same phases as seen in the methane flame under dry conditions, could be distinguished. Although under wet conditions, there is a shift in equivalence ratio. At ignition equivalence ratio ($\Phi = 0.8$, Figure 7(a)), the flame is located around the inner recirculation zone. Light emissions in the visible spectrum are shifted from blue to yellow. The flame is also slightly stretched, which was also noticed by Göke et al. (2012). Reducing the equivalence ratio results again in an oscillating flame ($\Phi = 0.65$). The flame oscillates between the inner and the outer recirculation zone (Figure 7(b)). Oscillations are however less violent than in the dry case, allowing fairly stable combustion. Steam has clearly a stabilizing effect on the methane combustion. This stabilizing effect is possibly due to the presence of additional OH or due to higher mass flow rate, which will affect the flame speed (Sayad et al., 2013). Finally, reducing the equivalence ratio

more ($\Phi = 0.57$) results in a stable, detached flame (Figure 7(c)). Reducing the equivalence ratio further will finally lead to blowout.

As a final remark, it is worth noting that steam has a very corrosive effect on the quartz tube of the burner. The steam affects the glass, by making it rough, resulting in a milky shine, which effects the photographs. During the experiments, no issues with condensation were experienced. However, at high steam fractions (28 %) droplets formed on the exhaust system of the combustion chamber, on the water-cooled metal liner (Figure 3). This condensation had no effect on the LBO limit.

3.2. *Impact of steam dilution on CO emissions*

CO levels in the exhaust gases start to rise for both swirl numbers ($S = 0.66$ and $S = 0.53$) at higher equivalence ratios with increasing steam fraction (Figure 8). This is a result of the higher LBO equivalence ratio. Measuring CO levels for decreasing equivalence ratios for pure methane combustion (no steam addition) was not possible. As mentioned before, at the transition zone where the flame evolves from a flame concentrated around the inner recirculation zone to a flame concentrated around the outer recirculated zone, the combustion became too unstable, resulting in blowout due to these instabilities. Therefore it was not possible to measure the exhaust gas emissions over a 3 minutes time period. For the determination of the LBO limit, the equivalence ratio was lowered faster, in order to go faster through this transition zone. After this transition zone, combustion was again stable, however CO levels were above the scale of the measuring device ($\geq$ 950 ppm). The instabilities at decreased equivalence ratio for methane combustion were less aggressive during steam injection. Therefore it was possible to capture CO levels at the transition zone.

At full combustion with a flame concentrated around the inner recirculation zone, CO levels are of the same order of magnitude as the pure methane combustion for

all steam fractions (Table 1). This indicates that the combustion is complete, which will result in a high combustion efficiency. $\Phi_{\text{transition}}$ from Table 1 is defined as the lowest equivalence ratio at which the flame is still concentrated around the inner recirculation zone. With increasing steam fraction, this $\Phi_{transition}$ shifts towards higher equivalence ratios. This shift is comparable to the shift in Φ_{LBO}. Therefore, full combustion occurs at higher equivalence ratio. This indicates that more fuel needs to be added to the combustion chamber under steam injection conditions.

Since CO levels were low, we can conclude that full, stable combustion was still achieved at steam fractions of 28 % ($S = 0.66$) and 18 % ($S = 0.53$). Higher steam fractions were not possible due to the limited power of the steam generator. Hermann et al. (2003) indicated that the maximum humidity level is dependent on inlet air temperature and aerodynamic load. In their experiments, the maximum achieved humidity level was 33 %. Above 33 %, CO levels become too high. Belokon et al. (2002) measured a high combustion efficiency at 20 % steam injection. The experimental results presented in this paper are in line with both studies.

3.3. *Effect of humidification on the performance of the mGT combustor*

By expressing the combustion efficiency as a function of the air mass flow rate, the rate of reaction, evaporation and mixing, Lefebvre (1998) has shown that with a limited number of experimental results the combustion efficiency of a GT combustor can be estimated over a wide operating range. For both the mGT combustor and the variable swirl, atmospheric combustion chamber used in the experiments of this paper, the fuel is gaseous and premixed and therefore the combustion efficiency can be assumed to be reaction controlled for both burners. Therefore, the expression of efficiency, provided by Lefebvre (1998), can be simplified to the

so-called 'theta'-parameter or 'air loading'-parameter to correlate efficiency.

$$\theta = \frac{p_{\text{in}}^{1.75} V_c \exp\left(\frac{T_{\text{in}}}{300}\right)}{\dot{m}_{\text{air}}} (Lefebvre,\ 1998). \tag{6}$$

By using this 'theta'-parameter, it is possible to use experimental obtained efficiencies from tests performed on lab scale test rigs (commonly at atmospheric pressure) to estimate the combustor efficiency under real operating conditions (at elevated pressure) when the combustor is installed in an actual test rig.

Depending on the load of the mGT (the mGT is operated at constant power output conditions by changing the rotational speed), inlet conditions vary when changing the power output. For different power outputs, ranging from 50 to 100 kW_e the air mass flow rate $\dot{m}_{\text{air}}$ changes from 0.578 to 0.737 kg/s, the inlet pressure of the combustor p_{in} from 3.30 to 4.34 bar, while the Combustor Inlet Temperature (CIT) remains more or less constant (a small reduction from 595 to 590 °C). When switching to humidified mode, part of the air mass flow rate is replaced by water, resulting in a lower rotational speed under constant power output conditions (De Paepe, Delattin, Bram and De Ruyck, 2012). This results in a reduced mass flow rate to the combustion chamber and lower inlet pressure. The changes in CIT are however again limited due to the good off-design behaviour of the recuperator. This results in the following conditions for the mGT converted into mHAT: for power output ranging from 50 to 100 kW_e, the air mass flow rate $\dot{m}_{\text{air}}$ changes from 0.500 to 0.609 kg/s, the inlet pressure of the combustor p_{in} from 3.14 to 4.00 bar and CIT from 590 to 578 °C. During dry operation, the equivalence ratio varies from 0.38 to 0.48, while during wet operation, the equivalence ratios is slightly higher (0.41 to 0.51) since more fuel needs to be burned to reach the same Turbine Outlet Temperature (TOT) (645 °C) due to the presence of water. At full humidification, the water fraction Ω ranges from 6.5 to 7.2 % for constant power outputs from 50 to 100 kW_e. Both dry and wet conditions of the Turbec T100 mGT obtained from Aspen® simulations (De Paepe et al., 2013).

Comparing the results of the experiments presented in this paper, with the operating range of the T100 combustor, indicates that the calculated values for the 'theta'-parameters are in the same range (Figure 9). This indicates that similar combustion efficiencies can be expected between the variable-swirl burner and the Turbec T100 combustion chamber. Since it was possible to get full, stable combustion with low CO emissions levels in the atmospheric test rig, however at higher equivalence ratios compared to dry operation, similar results can be expected for the T100 combustor. Since the mHAT operates already at higher equivalence ratio, no initial adaptations needed to be done to the fuel controller of the T100 combustor to reach stable combustion. This assumption was confirmed by humidified mGT experiments resulting in stable mGT operation at full humidification without modifying the fuel control set by the manufacturer (De Paepe, Carrero, Bram and Contino, 2015).

4. Numerical simulation models

As an extension to the conducted experiments, additional numerical simulations concerning the adiabatic flame temperature (equilibrium calculations) and the CO emission levels (equilibrium and chemical kinetics simulations) have been performed. The equilibrium calculations have been performed in `GASEQ` (Morley, 2005), while the chemical kinetics calculations where performed in `OpenSMOKE++` (Cuoci, Frassoldati, Faravelli and Ranzi, 2015) using a Perfectly Stirred Reactor (PSR). Simulations have been performed at different steam injection ratios and equivalence ratios.

4.1. *Equilibrium Calculations*

Increasing the steam injection ratio will lower the adiabatic flame temperature for corresponding equivalence ratios (Figure 10). As could be expected, the additional

steam in the combustion air will absorb heat generated by the combustion, resulting in a lower adiabatic flame temperature. To reach the same constant temperature, a higher equivalence ratio is necessary at higher steam fractions. The simulations presented in Figure 10 are generated using the same equivalence ratios and steam fractions as measured during the experiments presented in Figure 8. The swirl number was kept constant at 0.66.

Additionally to the adiabatic flame temperatures, the CO emissions at equilibrium have been calculated and compared to measurement results (Figure 10). For low steam flow rates and high equivalence ratios, the calculation results fit with the experimental results, however for high steam flow rates (23 %), the simulation results differ from the experimental results. Calculated CO values from CO_2dissociation at high temperature are much higher than the quantities we measured. This indicates that the emissions were measured at a much lower temperature than the adiabatic flame temperature. The lower flame temperature can be explained by the heat losses from the combustion chamber to the surroundings. The different results of the CO emissions when approaching the LBO indicate that this is a kinetic effect, rather than a temperature effect. Since `GASEQ` only allows equilibrium calculations, actual kinetic calculations (in `OpenSMOKE++`) were performed to simulate this effect (see next subsection).

Finally, the theoretic adiabatic flame temperature at the LBO limit has been calculated (Figure 11). The adiabatic flame temperature at LBO limit increases with increasing steam fraction. This indicates that next to the dilution effect (water absorbs heat, which should be compensated by a higher equivalence ratio), water has an additional effect on the flame speed, which results in blowout (causing the higher adiabatic flame temperature at higher steam fractions).

4.2. *Chemical kinetics calculations*

Additional chemical kinetic simulations were performed, using OpenSMOKE++. The idea is to show the importance of the kinetics in the final CO emissions in a qualitative way. We aimed to reproduce the specific CO emissions profile with these chemical kinetic simulations in a qualitative way, rather than to get a full validation of the measured emissions. The very accurate simulation of the combustion chamber was not within the scope of this paper. The combustion chamber was simulated as a PSR with a constant residence time. The residence time was kept constant at 2 s, which was calculated from the volumetric flow rate and the volume of the chamber. In these calculations, temperature was also kept constant and no energy calculations were performed. The temperature was calculated by taking the average of the inlet temperature and the expected flame temperature, taking into account the combustion efficiency. Finally, the GRI-Mech 3.0 for modelling of natural gas combustion from Berkeley, University of California has been used, since it has been optimized for methane and natural gas as fuel (Berkeley, University of California, 2000).

The simulations using OpenSMOKE++ indicate that it is possible to reproduce the specific profile of the CO emissions in a qualitative way (Figure 12). CO emissions are low when complete combustion occurs. When lowering the equivalence ratio by reducing the fuel flow rate, CO emissions start to rise due to a decreasing combustion temperature in combination with a limited reaction time. This effect can only be simulated when the kinetics are also taken into account, since simulations at the same temperature, with a much larger residence time (10 000 s) show different results (Figure 13). At higher equivalence ratios, the CO emissions increase due to dissociation of the CO_2 as a result of the high temperature. The difference between the results at large residence time (Figure 13) and the GASEQ results (Figure 10) can be explained by the difference in temperature. For the OpenSMOKE++ simulations, an average temperature was calculated and used, while GASEQ uses the adiabatic

flame temperature, which is much higher, resulting in more CO_2 dissociation.

The results of the OpenSMOKE++ simulations do not match perfectly with the measured results (Figure 12). This requires a much more detailed model of the combustion chamber than the PSR. To match simulations and experiments, the kinetics needs to be simulated in combination with the fluid mechanics, especially to simulate the effect of the recirculation zone, which affects the residence time of the different chemical species. As mentioned before, a full kinetic analysis of the combustion was however not within the scope of this paper.

5. Conclusion of combustion experiments

Steam dilution experiments have been conducted on an atmospheric, variable-swirl premixed combustor to study the effect of humidified combustion air on the CO emissions and LBO limit for methane combustion. The major conclusions from these experiments were:

- The LBO equivalence ratio increases linearly with increasing steam fraction.
- The CO levels start to rise at higher equivalence ratios when injecting more steam.
- CO levels at complete, stable humid combustion are constant and equal to those of dry combustion.
- Steam has a stabilizing effect on methane combustion when lowering the equivalence ratio.

Summarizing for mGT applications, it is possible to maintain a stable and complete combustion under steam injection conditions. However equivalence ratio needs to be increased in order to stay away from LBO limit and to keep CO emissions low.

6. Acknowledgement

This work was funded by the Research Foundation Flanders (FWO) and the Swedish Centre for Combustion Science and Technology (CeCOST).

Acronyms

CHP	Combined Heat and Power
CIT	Combustor Inlet Temperature
GT	Gas Turbine
HAT	Humid Air Turbine
ICE	Internal Combustion Engine
LBO	Lean Blowout
LDA	Laser Doppler Anemometry
mGT	micro Gas Turbine
mHAT	micro Humid Air Turbine
PSR	Perfectly Stirred Reactor
TOT	Turbine Outlet Temperature
VUB	Vrije Universiteit Brussel

Roman Symbols

G_a	axial flux of axial momentum	$\mathrm{kg\,m/s^2}$
G_t	axial flux of tangential momentum	$\mathrm{kg\,m^2/s^2}$
$\dot{m}$	mass flow rate	kg/s
p	pressure	Pa
R_S	radius of the swirler	m
r	radius of the swirler exit	m

S	Swirl number	
T	temperature	°C
U	axial velocity combustion air	m/s
V_c	volume of the combustion chamber	m^3
W	tangential velocity combustion air	m/s

Greek Symbols

Φ	equivalence ratio	
Ω	steam fraction	
ρ	density	kg/m^3
θ	theta parameter or air loading parameter	

Subscripts

air	properties of air
dry	dry condition
fuel	fuel
in	inlet condition
init	initial condition
steam	properties of steam

References

Belokon, A.A., Khritov, K.M., Klyachko, L.A., Tschepin, S.A., Zakharov, V.M., George Opdyke, J.. Prediction of combustion efficiency and NO_x levels for diffusion flame combustors in HAT cycles. In: ASME Conference Proceedings. ASME paper GT2002-30609; 2002. p. 791–797.

Berkeley, University of California, . Gri-mech 3.0. 2000. Online available: http://combustion.berkeley.edu/gri-mech/index.html (accessed: 10-11-2015).

Bhargava, A., Colket, M., Sowa, W., Casleton, K., Maloney, D.. An experimental and modeling study of humid air premixed flames. Journal of Engineering for Gas Turbines and Power 2000;122(3):405–411.

Cadorin, M., Pinelli, M., Vaccari, A., Calabria, R., Chiariello, F., Massoli, P., Bianchi, E.. Analysis of a micro gas turbine fed by natural gas and synthesis gas: MGT test bench and combustor CFD analysis. Journal of Engineering for Gas Turbines and Power 2012;134(7):071401 (11 pages).

Calabria, R., Chiariello, F., Massoli, P., Reale, F.. Cfd analysis of turbec t100 combustor at part load by varying fuels. In: ASME Turbo Expo 2015: Turbine Technical Conference and Exposition. American Society of Mechanical Engineers; GT2015-43455; 2015. p. V008T23A020–V008T23A020.

Cameretti, M.C., Piazzesi, R., Reale, F., Tuccillo, R.. Combustion simulation of an exhaust gas recirculation operated micro-gas turbine. Journal of Engineering for Gas Turbines and Power 2009;131(5):051701 (10 pages).

Cameretti, M.C., Reale, F., Tuccillo, R.. Cycle optimization and combustion analysis in a low-nox micro-gas turbine. In: ASME Conference Proceedings. ASME; volume 2006; 2006. p. 53–64.

Cameretti, M.C., Tuccillo, R.. Combustion analysis in a micro-gas turbine supplied with bio-fuels. In: ASME Conference Proceedings. ASME paper GT2014-25560; 2014. p. 12 pages.

Chen, A.G., Maloney, D.J., Day, W.H.. Humid air NO_x reduction effect on liquid fuel combustion. Journal of Engineering for Gas Turbines and Power 2004;126(1):69–74.

Cuoci, A., Frassoldati, A., Faravelli, T., Ranzi, E.. Opensmoke++: An object-oriented framework for the numerical modeling of reactive systems with detailed

kinetic mechanisms. Computer Physics Communications 2015;192:237 – 264.

Day, W., Kendrick D Knight, B., Bhargava, A., Sowa, W., Colket, M., Casleton, K., Maloney, D.. HAT cycle technology development program. In: Advanced turbine systems annual program review meeting. 1999. p. 2–8. Online available: www.netl.doe.gov/publications/proceedings/99/99ats/2-8.pdf (accessed: 23-01-2014).

De Paepe, W., Carrero, M.M., Bram, S., Contino, F.. T100 micro gas turbine converted to full humid air operation: A thermodynamic performance analysis. In: ASME Turbo Expo 2015: Turbine Technical Conference and Exposition. American Society of Mechanical Engineers; 2015. p. V003T06A015–V003T06A015.

De Paepe, W., Delattin, F., Bram, S., De Ruyck, J.. Steam injection experiments in a microturbine – A thermodynamic performance analysis. Applied Energy 2012;97:569 – 576.

De Paepe, W., Delattin, F., Bram, S., De Ruyck, J.. Water injection in a micro gas turbine – Assessment of the performance using a black box method. Applied Energy 2013;112:1291–1302.

Delattin, F., Bram, S., Knoops, S., De Ruyck, J.. Effects of steam injection on microturbine efficiency and performance. Energy 2008;33(2):241 – 247.

Dryer, F.. Water addition to practical combustion systemsâĂŤconcepts and applications. Symposium (International) on Combustion 1977;16(1):279 – 295.

Frost & Sullivan, . Combined heat and power: Integrating biomass technologies in buildings for efficient energy consumption. 2011.

Göke, S., Füri, M., Bourque, G., Bobusch, B., Göckeler, K., Krüger, O., Schimek, S., Terhaar, S., Paschereit, C.O.. Influence of steam dilution on the combustion of natural gas and hydrogen in premixed and rich-quench-lean combustors. Fuel Processing Technology 2013;107:14 – 22.

Göke, S., Schimek, S., Terhaar, S., Reichel, T., Göckeler, K., Krüger, O., Fleck, J., Griebel, P., Paschereit, C.O.. Influence of pressure and steam dilution on

NO_x and CO emissions in a premixed natural gas flame. In: ASME Conference Proceedings. ASME paper GT2013-94782; 2012. p. 11 pages.

Hermann, F., Klingmann, J., Gabrielsson, R.. Computational and experimental investigation of emissions in a highly humidified premixed flame. In: ASME Conference Proceedings. ASME paper GT2003-38337; 2003. p. 819–827.

Kobayashi, H., Yata, S., Ichikawa, Y., Ogami, Y.. Dilution effects of superheated water vapor on turbulent premixed flames at high pressure and high temperature. Proceedings of the Combustion Institute 2009;32(2):2607 – 2614.

Lefebvre, A.. GAS Turbine Combustion, Second Edition. Combustion: An International Series. Taylor & Francis, 1998.

Mazas, A.N., Lacoste, D.A., Schuller, T.. Experimental and numerical investigation on the laminar flame speed of CH_4/O_2 mixtures diluted with CO_2 and H_2O. In: ASME Conference Proceedings. ASME paper GT2010-22512; 2010. p. 411–421.

McDonald, C.F.. Low-cost compact primary surface recuperator concept for microturbines. Applied Thermal Engineering 2000;20(5):471 – 497.

Morley, C.. GASEQ: A chemical equilibrium program for windows. 2005. Online available: `http://www.gaseq.co.uk/` (accessed: 29-10-2015).

Parente, J., Traverso, A., Massardo, A.F.. Micro humid air cycle: Part B – Thermoeconomic analysis. In: ASME Conference Proceedings. ASME paper GT2003-38328; 2003. p. 231–239.

Park, J., Keel, S.I., Yun, J.H.. Addition effects of H_2 and H_2O on flame structure and pollutant emissions in methane-air diffusion flame. Energy & Fuels 2007;21(6):3216–3224.

Pilavachi, P.A.. Mini- and micro-gas turbines for combined heat and power. Applied Thermal Engineering 2002;22(18):2003 – 2014.

Sayad, P., Schönborn, A., Clerini, D., Klingmann, J.. Experimental investigation of methane lean blowout limit; effects of dilution, mass flow rate and inlet temperature. In: ASME Conference Proceedings. ASME paper GTINDIA2012-

9742; 2012. p. 815–826.

Sayad, P., Schönborn, A., Klingmann, J.. Experimental investigations of the lean blowout limit of different syngas mixtures in an atmospheric, premixed, variable-swirl burner. Energy & Fuels 2013;27(5):2783–2793.

Sayad, P., Schönborn, A., Li, M., Klingmann, J.. Visualization of different flashback mechanisms for H_2/CH_4 mixtures in a variable-swirl burner. In: ASME Conference Proceedings. ASME paper GT2014-27090; 2014. p. 11 pages.

Syred, N., Beér, J.. Combustion in swirling flows: A review. Combustion and Flame 1974;23(2):143 – 201.

Turbec AB, . T100 microturbine CHP system: Technical description ver 4.0; 2000-2001. .

U.S. Department of Energy, Office of Energy Efficiency & Renewable Energy, Office of Power Technologies, . Advanced microturbine systems – Program plan for fiscal years 2000 through 2006. 2000. Online available: `http://www.energetics.com/resourcecenter/products/plans/samples/Documents/advanced_microturbine_plan.pdf` (accessed: 14-09-2014).

Xiao, W., Huang, Y.. Lean blowout limits of a gas turbine combustor operated with aviation fuel and methane. Heat and Mass Transfer 2015;:1–10.

Zhao, D., Yamashita, H., Kitagawa, K., Arai, N., Furuhata, T.. Behavior and effect on NO_x formation of OH radical in methane-air diffusion flame with steam addition. Combustion and Flame 2002;130(4):352 – 360.

Table 1. CO levels are constant and independent of the steam flow rate in full combustion conditions.

$\Omega(\%)$	$\Phi_{transition}$	CO (ppm)
0	0.48	40
10.6	0.53	41
17.7	0.65	40
22.6	0.75	31
28.3	0.85	41

Figure 1. Combustion chamber of the Turbec T100 mGT dismounted from the test rig at the VUB.

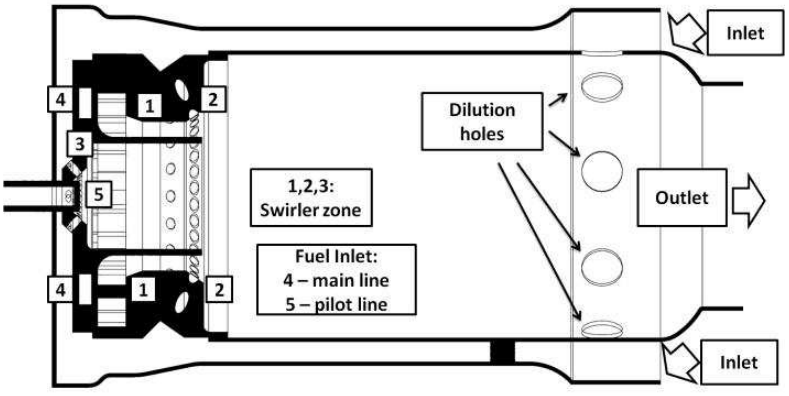

Figure 2. Turbec T100 combustor scheme indicating the different parts (Calabria et al., 2015)

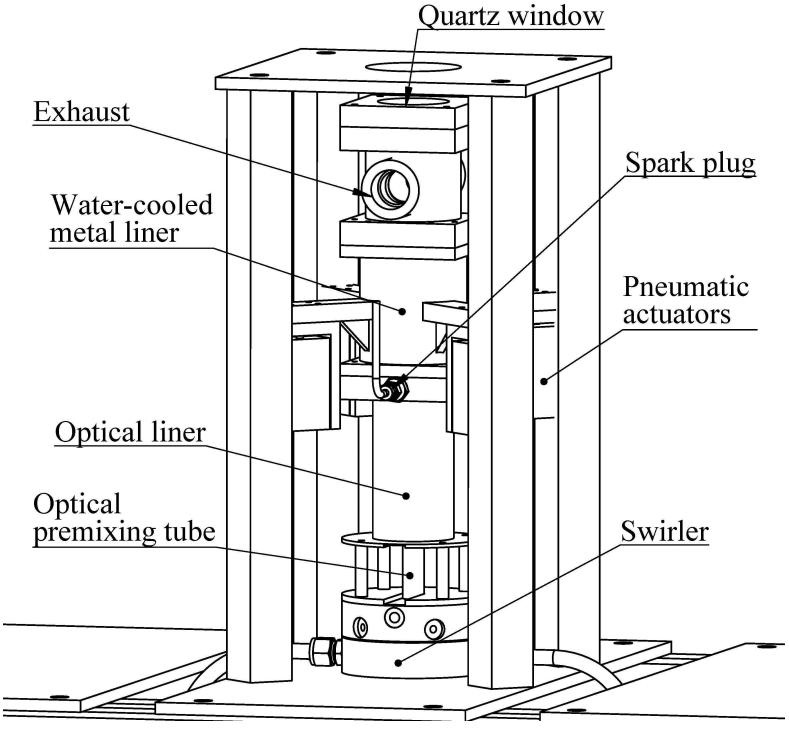

Figure 3. The variable-swirl burner, at the labs of the Thermal Power Engineering division of the Department of Energy Sciences of Lund University, Sweden, has an optical access to study the flames (Sayad et al., 2014).

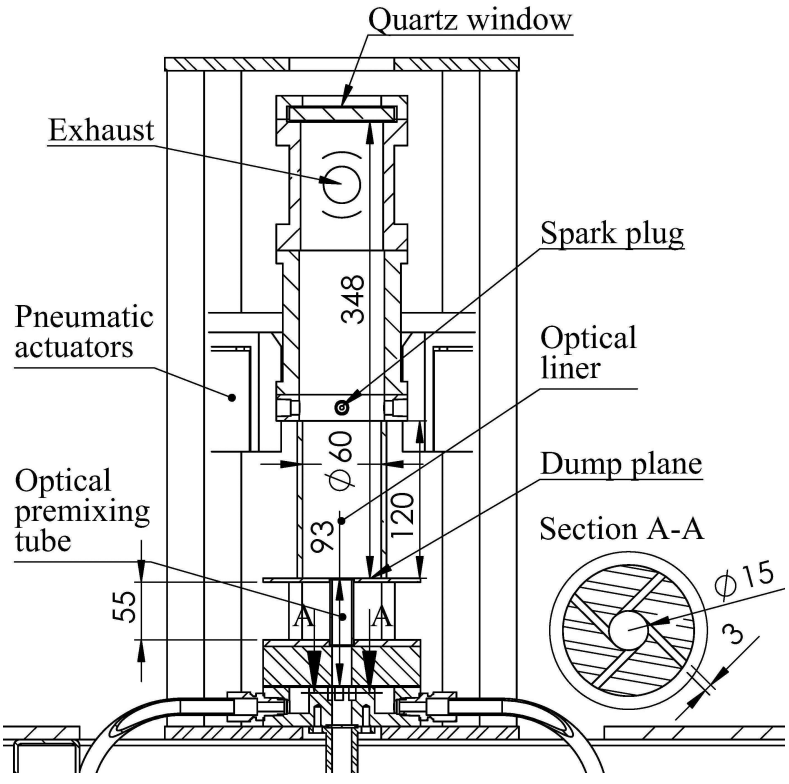

Figure 4. Cross section of the swirler (Sayad et al., 2014).

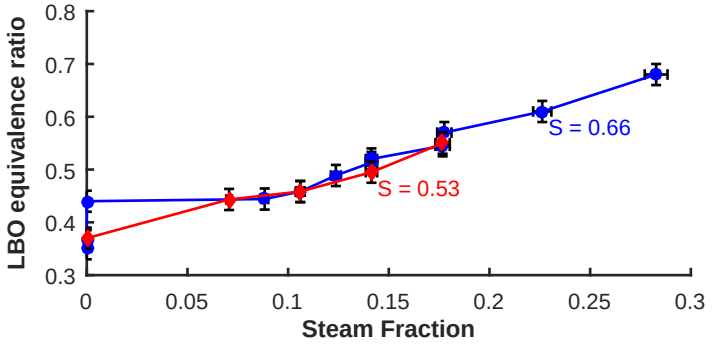

Figure 5. The LBO equivalence ratio increases linearly with increasing steam fraction in the combustion air.

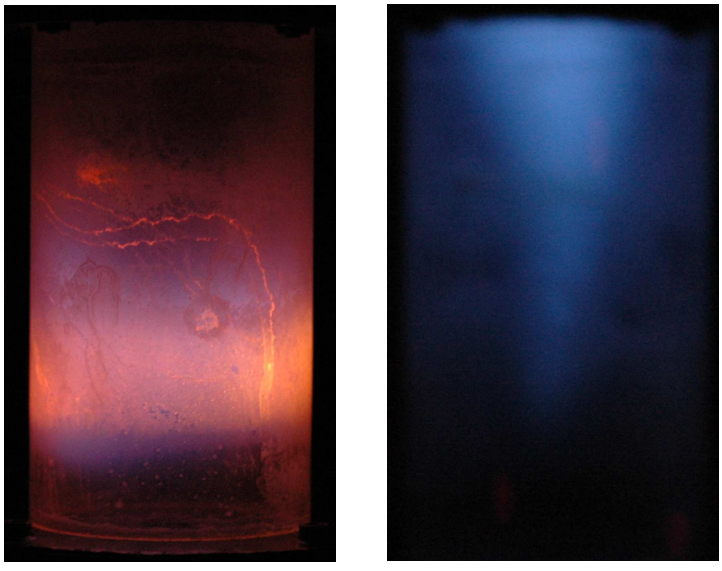

(a) (b)

Figure 6. Broadband luminosity photographs of a methane flame at $S = 0.53$, no steam injection and $\Phi = 0.5$ (a) and $\Phi = 0.38$ (b).

(a) (b) (c)

Figure 7. Broadband luminosity photographs of a methane flame at $S = 0.53$, with steam injection of 2.5 kg/h ($\Omega = 18\,\%$) and $\Phi = 0.8$ (a), $\Phi = 0.65$ (b) and $\Phi = 0.57$ (c).

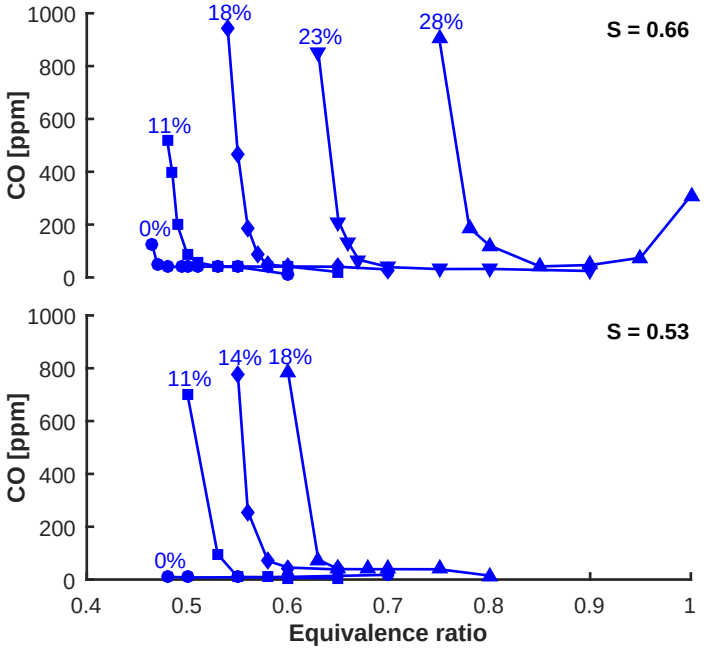

Figure 8. CO levels increase with decreasing equivalence ratio. At high steam fraction, CO levels are still low which indicate that the combustion efficiency remains high.

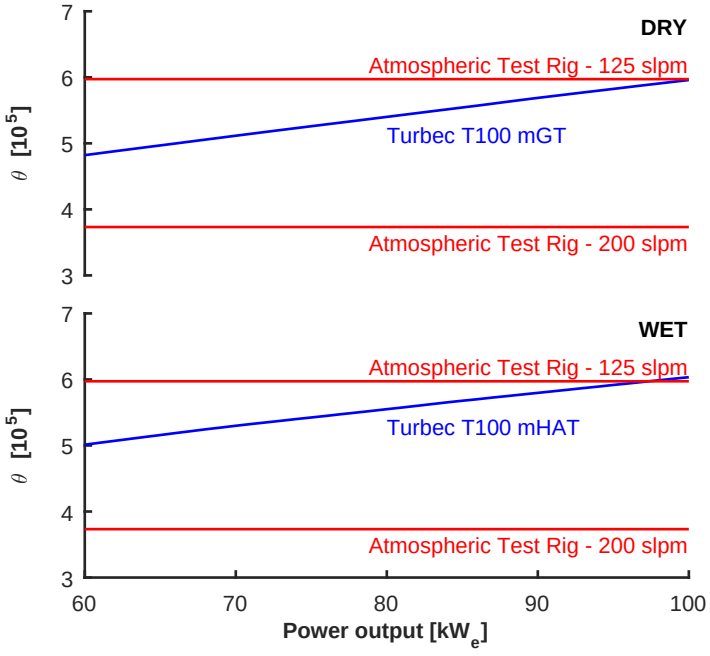

Figure 9. For both dry and wet mGT operations, the calculated 'theta'-parameters ((Lefebvre, 1998)) match with the used ranges during the experiments presented in this paper.

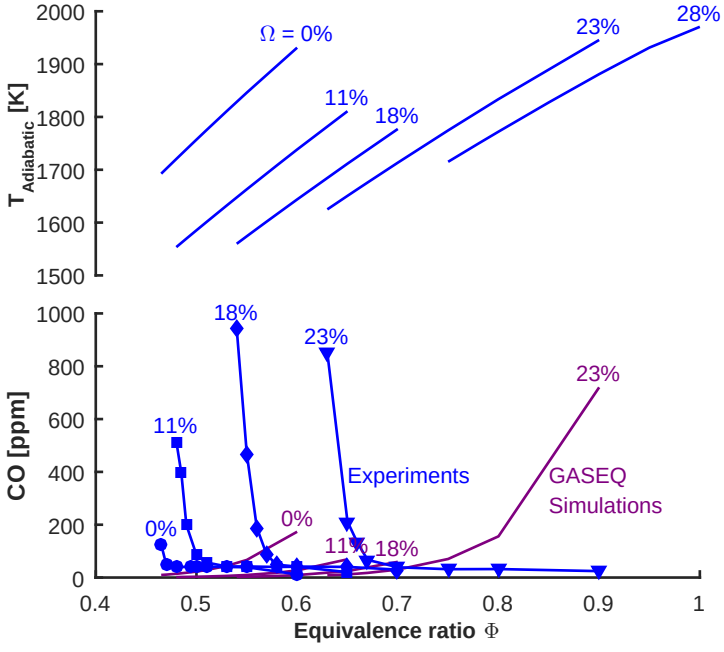

Figure 10. For constant equivalence ratios and increasing steam fractions, the simulated adiabatic flame temperature is increases due to the higher heat absorption by the steam.

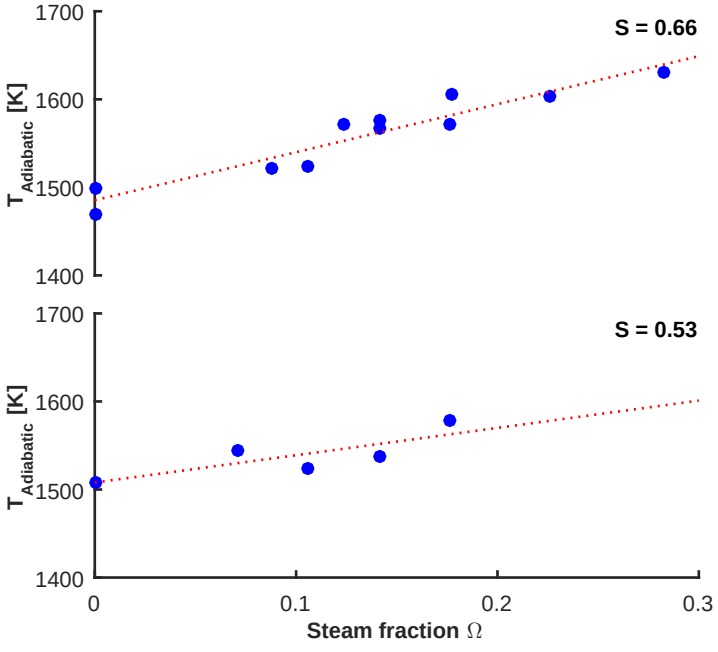

Figure 11. The adiabatic flame temperature at LBO limit increase with increasing steam fraction, which indicates that next to the dilution effect, water has an additional effect on the flame speed, resulting in blowout.

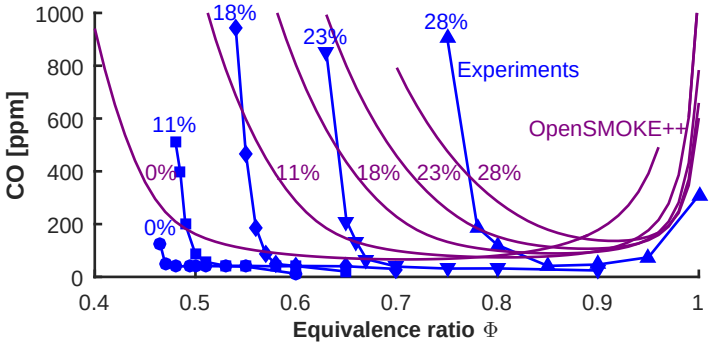

Figure 12. Chemical kinetics simulations performed in `OpenSMOKE++` using a PSR model of the combustion chamber show the increasing CO emission levels when approaching the LBO limit due to a reducing flame temperature. At high equivalence ratios, the CO emission levels increase due to the dissociation of the CO_2 at higher temperature. CO emissions do not match perfectly, since the PSR is a rouch approximation of the burner.

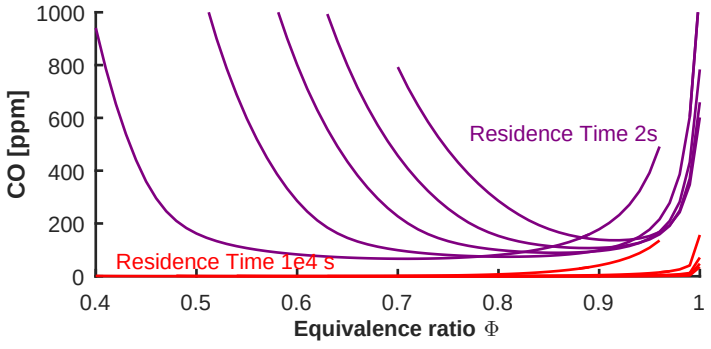

Figure 13. Chemical kinetics simulations performed in `OpenSMOKE++` using residence times of 2 s and 10 000 s illustrate that the increasing CO emission levels at equivalence ratios close to the LBO limit are a results of the reducing temperature in combination with the chemical kinetics.